J|A|C|S
ARTICLES
Published on Web 05/26/2007

Polyethylene Imine Derivatives ('Synzymes') Accelerate Phosphate Transfer in the Absence of Metal

Frédéric Avenier, Josiel B. Domingos,† Liisa D. Van Vliet, and Florian Hollfelder*

Contribution from the Department of Biochemistry, University of Cambridge, Cambridge CB2 1GA, United Kingdom

Received December 19, 2006; E-mail: fh111@cam.ac.uk

Abstract: The efficient integration of binding, catalysis, and multiple turnovers remains a challenge in building enzyme models. We report that systematic derivatization of polyethylene imine (PEI) with alkyl ($C_{2-}C_{12}$), benzyl, and guanidinium groups gives rise to catalysts ('synzymes') with rate accelerations (k_{cat}/k_{uncat}) of up to 10^4 for the intramolecular transesterification of 2-hydroxypropyl-*p*-nitrophenyl phosphate, HPNP, in the absence of metal. The synzymes exhibit saturation kinetics ($K_M \approx 250\ \mu M$, $k_{cat} \approx 0.5\ min^{-1}$) and up to 2340 turnovers per polymer molecule. Catalysis can be specifically and competitively inhibited by anionic and hydrophobic small molecules. The efficacy of catalysis is determined by the PEI derivatization pattern. The derivatization reagents exert a synergistic effect, i.e., their combinations increase catalysis by more than the sum of each single modification. The pH−rate profile for k_{cat}/K_M is bell shaped with a maximum at pH 7.85 and can be explained as a combination of two effects that both have to be operative for optimal activity: K_M increases at high pH due to deprotonation of PEI amines that bind the anionic substrate and k_{cat} decreases as the availability of hydroxide decreases at low pH. Thus, catalysis is based on substrate binding by positively charged amine groups and the presence of hydroxide ion in active sites in an environment that is tuned for efficient catalysis. Inhibition studies suggest that the basis of catalysis and multiple turnovers is differential molecular recognition of the doubly negatively charged transition state (over singly charged ground state and product): this contributes a factor of at least 5−10-fold to catalysis and product release.

Introduction

Phosphate transfer is one of the most common bioreactions but also one of the thermodynamically most demanding.[1] Nature has developed two general strategies to accelerate the hydrolysis of phosphate esters. On one hand, metal-ion cofactors can be recruited into enzyme active sites in a characteristic structural motif consisting of two divalent metal ions[2−4] to provide substrate binding, activation of the nucleophile (by pK_a lowering), and Lewis acid catalysis. On the other hand, enzymes such as RNase A lack metal ions but achieve similar rate accelerations for phosphate diester cleavage using hydrogen bonding and general acid−base catalysis alone.[5] While a large number of metal-based enzyme models show remarkable efficiency,[6−8] very few metal-free artificial catalysts have been described (see Table 1) with rate accelerations k_{cat}/k_{uncat} well below 500 and limited to a single turnover: a cyclodextrin with pendant imidazole groups as bifunctional general acid−base catalysts,[9] a bisguanidinium receptor,[10] a sapphyrin derivative,[11] and simple guanidinium compounds with lowered pK_a values to act as general acids.[12,13] Each of these models provides functionality that is familiar from enzyme actives sites, but because of their small size, all lack the ability to shield the substrate from the aqueous environment and create a specific microenvironment. Modified polyethylene imines ('synzymes') are larger enzyme models (similar to dendrimers[14]) that derive their catalytic power from creating a medium resembling that of an enzyme active site when they bind substrates.[15−23] In the past we extended

† Permanent address: Departamento de Química, Universidade Federal de Santa Catarina, Florianópolis, SC, 88040-900, Brazil.

(1) Cleland, W. W.; Hengge, A. C. *Chem. Rev.* **2006**, *106*, 3252−78.
(2) Cowan, J. A. *Chem. Rev.* **1998**, *98* (3), 1067−1088.
(3) Steitz, T. A.; Steitz, J. A. *Proc. Natl. Acad. Sci. U.S.A* **1993**, *90* (14), 6498−502.
(4) Wilcox, D. E. *Chem. Rev.* **1996**, *96* (7), 2435−2458.
(5) Raines, R. T. *Chem. Rev.* **1998**, *98* (3), 1045−1066.
(6) Morrow, J. R.; Iranzo, O. *Curr. Opin. Chem. Biol.* **2004**, *8* (2), 192−200.
(7) Molenveld, P.; Engbersen, J. F. J.; Reinhoudt, D. N. *Chem. Soc. Rev.* **2000**, *29*, 75−86.
(8) Williams, N. H.; Takasaki, B.; Wall, M.; Chin, J. *Acc. Chem. Res.* **1999**, *32*, 485−493.
(9) Anslyn, E.; Breslow, R. *J. Am. Chem. Soc.* **1989**, *111*, 5972−5973.
(10) Jubian, V.; Veronese, A.; Dixon, R. P.; Hamilton, A. D. *Angew. Chem., Int. Ed. Engl.* **1995**, *34* (11), 1237−1239.
(11) Kral, V.; Lang, K.; Kralova, J.; Dvorak, M.; Martasek, P.; Chin, A. O.; Andrievsky, A.; Lynch, V.; Sessler, J. L. *J. Am. Chem. Soc.* **2006**, *128* (2), 432−437.
(12) Scheffer, U.; Strick, A.; Ludwig, V.; Peter, S.; Kalden, E.; Göbel, M. W. *J. Am. Chem. Soc.* **2005**, *127* (7), 2211−7.
(13) Piatek, A. M.; Gray, M.; Anslyn, E. V. *J. Am. Chem. Soc.* **2004**, *126* (32), 9878−9.
(14) Kofoed, J.; Reymond, J. L. *Curr. Opin. Chem. Biol.* **2005**, *9* (6), 656−64.
(15) Klotz, I. In *Enzyme Mechanisms*; Page, M. I., Williams, A., Eds.; The Royal Society of Chemistry: London, 1987; pp 14−34.
(16) Klotz, I. M.; Suh, J. In *Artificial Enzymes*; Breslow, R., Ed.; Wiley-VCH: Weinheim, 2005; pp 63−88.
(17) Suh, J. *Synlett* **2001**, *9*, 1343−1363.
(18) Liu, L.; Zhou, W.; Chruma, J.; Breslow, R. *J. Am. Chem. Soc.* **2004**, *126* (26), 8136−7.
(19) Liu, L.; Breslow, R. *J. Am. Chem. Soc.* **2002**, *124* (18), 4978−9.
(20) Liu, L.; Breslow, R. *Bioorg. Med. Chem.* **2004**, *12* (12), 3277−87.
(21) Liu, L.; Rozenman, M.; Breslow, R. *J. Am. Chem. Soc.* **2002**, *124* (43), 12660−1.

Table 1. Comparison of the Kinetic Parameters for Different Catalysts[a]

catalyst	substrate	metal	solvent	k_{cat} or k_1 [10^{-4} s^{-1}]	K_M [mM]	k_{cat}/K_M or k_2 [M^{-1} s^{-1}]	no. of turnovers	k_{cat}/k_{uncat}	catalytic proficiency[h]	ref
D9 whole polymer	HPNP		H_2O	84.5	0.25	33.8	2340	46 800[b]	1.8×10^8	*i*
per active site	HPNP		H_2O	6.5	0.25	2.6	180	3600[b]	1.4×10^7	*i*
bis(alkylguanidinium)	HPNP		MeCN	1.1	1.6	0.068	<1	290[c]	1.8×10^5	10
polyhydroxylated sapphyrin	BNPP		H_2O	0.0009	2.0	0.000045	1.2	20[d]	1×10^4	11
tris(2-aminobenzimidazoles)	RNA		H_2O				<1			12
cyclodextrins	BCCP		H_2O	14	0.18	7.8	<1	140[e]	7.8×10^5	9
calix[4]aren-2Zn	HPNP	Zn^{2+}	H_2O/MeCN	7.7	0.018	43	≥4	28 500[f]	1.5×10^9	43
calix[4]aren-3Zn	HPNP	Zn^{2+}	H_2O/MeCN	24	0.83	2.9	≥4	88 000[f]	1.0×10^8	43
nanozyme-*n*Zn	HPNP	Zn^{2+}	H_2O	42	0.93	4.4	≥100	150 000[f]	1.6×10^8	44
Synzyme-*n*Ni	HPNP	Ni^{2+}	H_2O	>10	>10	0.1	4	37 000[f]	3.7×10^6	45
dinuc. complex	HPNP	Zn^{2+}	H_2O	41	16	0.25	<1	120 000[g]	7.5×10^6	46
dinuc. complex	HPNP	Zn^{2+}	H_2O	170	0.32	53	10	1 000 000[g]	1.4×10^9	47

[a] HPNP (2-hydroxypropyl *p*-nitrophenyl phosphate), BNPP (bis-(4-nitrophenyl) phosphate), RNA (30−40-mer oligonucleotides), BCCP (4-*ter*-butylcatechol cyclic phosphate). [b] $k_{uncat} = 1.8 \times 10^{-7}$ s^{-1}. [c] $k_{uncat} = 3.8 \times 10^{-7}$ s^{-1}. [d] On the basis of the extrapolation of the measured rate k_{uncat}=1.1×10^{-10} s^{-1}; pH 6.6, 20 °C; (ref 48) to our conditions (pH 7.5 (×10), 37 °C (×4)), giving an extrapolated $k_{uncat} = 4.4 \times 10^{-9}$ s^{-1}. [e] $k_{uncat} = 1 \times 10^{-5}$ s^{-1} (ref 49). [f] $k_{uncat} = 2.7 \times 10^{-8}$ s^{-1} (ref 43). [g] $k_{uncat} = 3.8 \times 10^{-8}$ s^{-1} (ref 46). [h] $(k_{cat}/K_M)/k_{uncat}$ normalized to a concentration of 1 M catalyst. [i] This work.

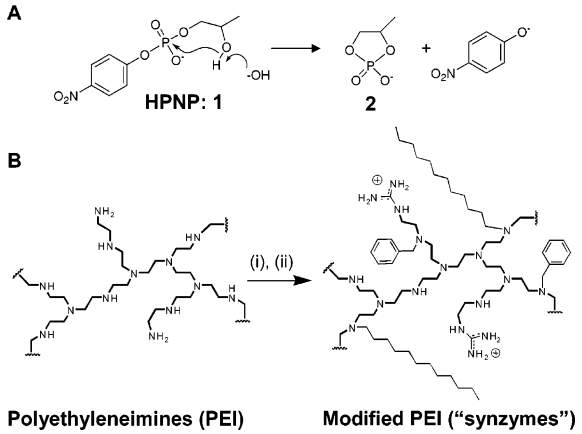

Figure 1. (A) HPNP transesterification reaction. (B) Derivatization scheme to modify PEI to give 'synzymes'. Polymer amine groups were reacted (in DMF, 30 °C) with varying amounts of (i) praxadine (1*H*-pyrazole-1-carboxamidine hydrochloride) (4 h) and (ii) iodoalkanes (C_2−C_{12}, see Figure 2A) or an equimolar mixture of iodododecane and benzylbromide (see Figure 2B) for 5 days.

the use of this approach by employing high-throughput derivatization with alkylation reagents (introducing methyl, dodecyl, and benzyl groups) to change the properties of PEI comprehensively, followed by screening to identify the best catalysts. For one prominent, medium-sensitive proton-transfer reaction from carbon−the Kemp elimination[24−27]—this protocol produced catalysts with rate accelerations k_{cat}/k_{uncat} up to 10^7.[28,29]

Now we seek to catalyze the thermodynamically more difficult transesterification reaction of phosphate diester **1** (HPNP, see Figure 1A)[30] in the absence of metal as a model for RNA cleavage. We mimic the active sites of many phosphatases that contain guanidinium groups[31,32] and add hydrophobic reagents to create a cluster of hydrophobic groups by way of emulating the interior of a protein. Figure 1B shows the derivatization chemistry used in this work to attach alkyl, benzyl, and guanidinium groups[33] to PEI. Several features of these modified PEIs suggest that they may also be capable of phosphate transfer catalysis: (i) a positively charged PEI framework (protonated and quaternized PEI amines as well as guanidinium groups) will attract the negatively charged substrate. Guanidinium groups which are familiar features of phosphatase active sites (e.g., ribonuclease A,[34] binase,[35] staphylococcal nuclease,[36,37] or alkaline phosphatases[38]) further introduce a specific phosphate recognition element. (ii) Protons and positively charged groups may offset negative charge development in the transition state. (iii) The hydrophobic character of the derivatization reagents and charges resulting from derivatization may bring about a suitable reaction medium that is different from water. Recent work on the metal-catalyzed reaction of HPNP[39] has shown that this reaction has the potential to be substantially accelerated by specific localized microenvironments.

It is not obvious in which proportions these ingredients have to be provided to create efficient catalysts, so we again used high-throughput derivatization to modify PEI followed by screening in situ in 96-well plates in the presence of the metal chelator EDTA. Analysis of 200 synzymes identified a synzyme catalyst that was able to catalyze the transesterification of HPNP in water in the absence of metal ions with a rate acceleration k_{cat}/k_{uncat} of 4.6×10^4. The catalyst shows saturation kinetics, 2340 turnovers per catalyst molecule, and catalysis can be specifically and competitively inhibited.

(22) Breslow, R.; Bandyopadhyay, S.; Levine, M.; Zhou, W. *Chembiochem* **2006**, *7* (10), 1491−6.
(23) Haimov, A.; Cohen, H.; Neumann, R. *J. Am. Chem. Soc.* **2004**, *126* (38), 11762−3.
(24) Casey, L. M.; Kemp, D. S.; Paul, K. G.; Cox, D. D. *J. Org. Chem.* **1973**, *38* (13), 2294−2301.
(25) Kemp, D. S.; Casey, M. L. *J. Am. Chem. Soc.* **1973**, *95*, 6670−6680.
(26) Kemp, D. S.; Cox, D. D.; Paul, K. G. *J. Am. Chem. Soc.* **1975**, 7312−7318.
(27) Kemp, D. S.; Paul, K. G. *J. Am. Chem. Soc.* **1975**, 7305−7312.
(28) Hollfelder, F.; Kirby, A. J.; Tawfik, D. S. *J. Am. Chem. Soc.* **1997**, *119*, 9578−9579.
(29) Hollfelder, F.; Kirby, A. J.; Tawfik, D. S. *J. Org. Chem.* **2001**, *66* (17), 5866−74.
(30) Brown, D. M.; Usher, D. A. *J. Chem. Soc.* **1965**, 6558−6564.
(31) Perreault, D. M.; Cabell, L. A.; Anslyn, E. V. *Bioorg. Med. Chem.* **1997**, *5* (6), 1209−20.
(32) Schug, K. A.; Lindner, W. *Chem. Rev.* **2005**, *105* (1), 67−114.
(33) Bernatowicz, M. S.; Wu, Y.; Matsueda, G. R. *J. Org. Chem.* **1992**, *57*, 2497−2502.
(34) Yakovlev, G. I.; Mitkevich, V. A.; Shaw, K. L.; Trevino, S.; Newsom, S.; Pace, C. N.; Makarov, A. A. *Protein Sci.* **2003**, *12* (10), 2367−73.
(35) Yakovlev, G. I.; Struminskaya, N. K.; Znamenskaya, L. V.; Kipenskaya, L. V.; Leschinskaya, I. B.; Hartley, R. W. *FEBS Lett.* **1998**, *428* (1−2), 57−8.
(36) Cotton, F. A.; Hazen, E. E., Jr.; Legg, M. J. *Proc. Natl. Acad. Sci. U.S.A.* **1979**, *76* (6), 2551−5.
(37) Serpersu, E. H.; Shortle, D.; Mildvan, A. S. *Biochemistry* **1987**, *26* (5), 1289−300.
(38) Coleman, J. E. *Annu. Rev. Biophys. Biomol. Struct.* **1992**, *21*, 441−83.
(39) Neverov, A. A.; Lu, Z. L.; Maxwell, C. I.; Mohamed, M. F.; White, C. J.; Tsang, J. S.; Brown, R. S. *J. Am. Chem. Soc.* **2006**, *128* (50), 16398−405.

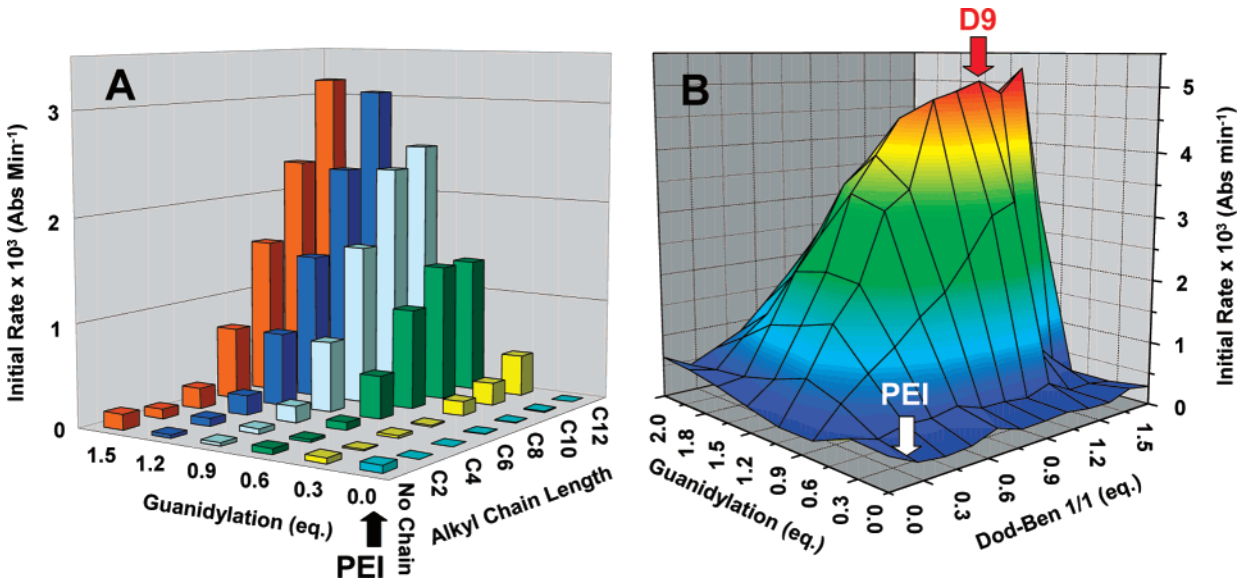

Figure 2. PEI modifications correlated to activity. PEIs were modified first by guanidylation, which is selective for primary amino groups, followed by addition of hydrophobic groups with C_2-C_{12} alkyl and/or benzyl groups (Figure 1B) and screened for the reaction shown in Figure 1A. (A) Screening results for a library in which the length of the alkyl chain was varied (no chain to C_{12}, 1 equiv per amino group) against the amount of guanidylation (0−1.5 equiv per primary amino group or 0−0.375 equiv per amino group). (B) Screening results for a library in which the amount of an equimolar mixture of dodecylation and benzylation groups was varied from 0 to 1.5 equiv per amino group and the amount of guanidylation was varied from 0 to 2 equiv per primary amino group (or 0 to 0.5 equiv per monomer). Quantities of modification reagent are plotted against the initial rates obtained in screening experiments in 96-well format. Each data point represents one synthesized polymer. Conditions: [HEPES] = 50 mM, [HPNP] = 1 mM, [synzyme] = 3 μM, 30 °C, pH 8.

Results

PEI Derivatization Brings About Efficient Catalysts. PEI modification was carried out in the same 96-well format as activity screening for the reaction **1** → **2** (Figure 1A). Figure 2 shows a representation of initial rates plotted as a function of the derivatization pattern brought about by PEI modification (Figure 1B). The underivatized PEI has little activity and is included for comparison in the origin of the plots. Variation of the length of the alkyl chain can result in a rate increase up to about 100-fold and guanidylation in a rate increase up to about 200-fold. These effects, however, are not independent of one another. For example, increasing the chain length to C_{12} has no effect if no guanidinium groups are present (Figure 2A). When 1.2 equiv of guanidinium per primary amino group are present, the same change results in a 95-fold increase. At the same time the effect of an increase in equivalents of guanidinium has a very small effect (2-fold) in the absence of alkyl groups (Figure 2A). However, in the presence of C_{10}, the increase is 193-fold: thus, the derivatization reagents exert a synergistic effect, i.e., combinations of derivatizations increase catalysis by up to two orders of magnitude more than the sum of each single modification. The increases in activity correlate smoothly with the changes in the composition of the derivatization mix and show that changes in the properties of the catalyst are a function of the amount of the derivatization reagents.

The observed effects validate our derivatization protocol in which a large number of reagent combinations can be efficiently screened. With regard to specific modifications that enhance catalysis, a chain of 12 carbons is optimal within the range of reagent combinations tested. We were unable to derivatize with longer carbon chains because the resulting PEI derivatives had limited solubility in water. To minimize solubility problems, we introduced benzyl groups, shown to confer improved solubility in previous work.[28,29] Figure 2B shows the results of a screening of libraries that contain equimolar mixtures of dodecyl and benzyl groups (as the hydrophobic component) in addition to the guanidinium groups. Just as in the case of the length of hydrophobic derivatization reagent, we observed synergy between guanidylation and the amount of alkylation. For example, in the absence of guanidylation there is no effect on rates as a result of addition of dodecyl and benzyl groups (1.05 equiv per amino group), but there is a marked 12-fold increase in activity upon hydrophobic derivatization when PEI has been previously derivatized with 1.2 equiv of guanidinium per primary amino group (relative to a PEI with dodecyl and benzyl groups only).

Kinetic Characterization of the Selected Catalyst. The best catalyst, D9, contains 0.9 equiv of guanidylation per primary amino group and 1.05 equiv of the equimolar alkylation mixture of dodecyl and benzyl groups per amino group (25% of the PEI amines are primary, 50% secondary, 25% tertiary[17]). For detailed study after initial screening, D9 was resynthesized on a larger scale, followed by purification by extensive dialysis.

Figure 3A shows a time course of the D9-catalyzed reaction compared to background (inset) and a Michaelis−Menten plot derived from initial rate measurements. Unlike underivatized PEI, D9 exhibits saturation behavior (with $K_M = 0.25$ mM and $k_{cat} = 0.0085$ s^{-1} at pH 7.85). Figure 3C shows that D9 is a true catalyst with up to 2340 turnovers per catalyst molecule as a lower limit, although turnover rate is eventually limited by product inhibition. The time courses, as well as the Michaelis−Menten data, remain unchanged in the presence of Chelex, demonstrating that no metal ions are required for catalysis. Chelex was also included during workup and dialysis as well as screening of D9. All handling of the synzymes during synthesis and kinetic measurements was carried out in plasticware, minimizing the possibility of metal-ion contamination,

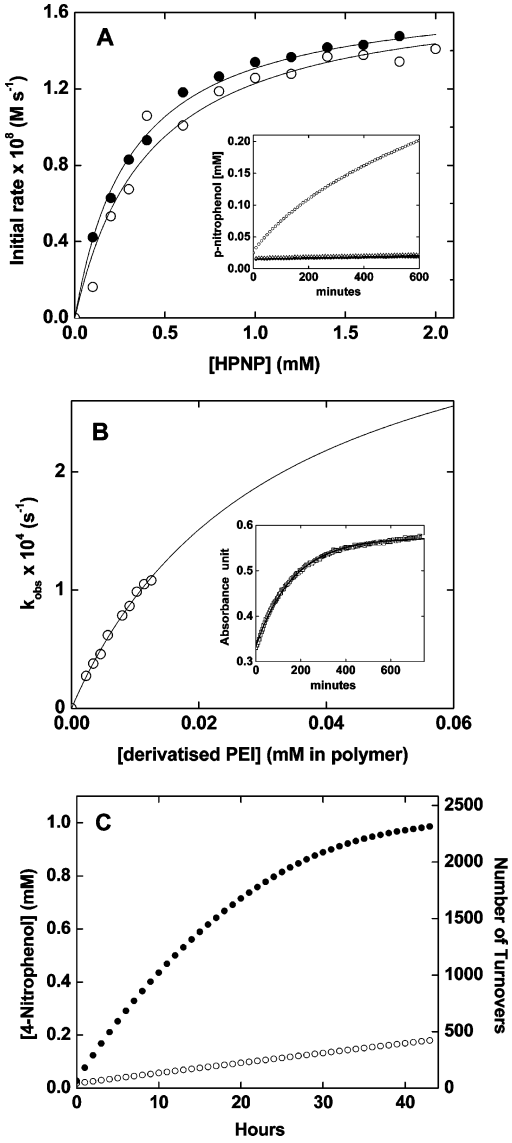

Figure 3. Polymer D9 exhibits saturation behavior consistent with the assumption of discrete active sites. (A) Initial rates v_0 exhibit saturation behavior in a Michaelis−Menten plot with an excess of substrate over enzyme ([synzyme] = 3.44 μM; [S] = 0−2 mM) with (○) and without (●) Chelex. (Inset) Time course of the synzyme-catalyzed reaction (○) in comparison to the reaction of underivatized PEI (△) and diethylenetriamine (●) catalyzed reaction. (B) Single-turnover kinetics for D9 with an excess of enzyme over substrate ([synzyme] = 0−12.6 μM; [S] = 25 μM). We show a notional fit to a reverse Michaelis−Menten equation (k_{obs}= $(k_{cat})^{site}[E_0]/([E_0] + K_M)$), although the large extrapolation leads to a large error in this fit. (Inset) Time courses under these conditions (e.g., here [synzyme] = 10 μM) were fit to a first-order exponential to give k_{obs} = 9.83×10^{-5} s^{-1}. (C) Time course to determine the number of turnovers in the reaction catalyzed by D9 (●) and background reaction (○). Conditions: [polymer] = 0.42 μM, [HPNP] = 1 mM, pH 7.85, 30 °C. The rate recedes to background after approximately 180 turnovers per site (or 2340 turnovers per polymer molecule).

e.g., from exposure to glassware. (Added metal ions exert an additional catalytic effect, demonstrating that potential metal binding sites are not saturated.[40])

The Michaelis−Menten parameters determined in Figure 3A sum up turnover of all active sites on the derivatized polymer. It is possible to determine the number of active sites per PEI molecule by measuring a $(k_{cat})^{site}$ [28,29,41] describing the activity per site under single turnover conditions ([synzyme] > [S]). Figure 3B shows a first-order reaction under these conditions (inset) that was fitted exponentially (to give a first-order rate constant k_{obs}) and a replot of k_{obs} against synzyme concentration, giving an extrapolated k_{cat} of 6.5×10^{-4} s^{-1}.[42] The number of active sites (given by the ratio between k_{cat} and $(k_{cat})^{site}$) is 13 and independent of pH around the optimum pH between 7.5 and 8.5 (see Figure S1), i.e. 45 $-(CH_2CH_2)NHR-$ monomers appear to form an active site. Extrapolation of k_{cat} to $(k_{cat})^{site}$ carries a large error because the data only deviate slightly from linearity, but the limited solubility precluded determination of k_{obs} at higher concentrations of D9, which naturally affects the quality of the fit. Therefore, extrapolation can only provide an upper limit for the active site concentration and a lower limit for $(k_{cat})^{site}$. However, data obtained in independent experiments and at various pH values (Supporting Information, Figure S1) lead to similar extrapolated values for $(k_{cat})^{site}$.

Rate Accelerations. The selected synzyme catalyst is an extraordinarily efficient phosphate transfer catalyst. Table 1 lists the measured quantitative parameters for D9 and their comparison to background rates. D9 shows a rate enhancement k_{cat}/k_{uncat} of 46 800 for the whole polymer (and of 3600 for a single 'active site' using $(k_{cat})^{site}$) over the background hydrolytic activity (measured as $k_{uncat} = 1.8 \times 10^{-7}$ s^{-1} at pH 8).

For calculation of the catalytic proficiency $(k_{cat}/K_M)/k_2$, a second-order rate constant k_2 was calculated from k_{uncat} by assuming a normalized concentration of 1 M catalyst (giving a formal k_2 of 1.8×10^{-7} s^{-1} M^{-1}), as has been done for comparison of other models.[46] The catalytic proficiency so obtained was 1.8×10^8 M^{-1} overall and 1.4×10^7 M^{-1} per site. The value of the hypothetical transition-state binding constant K_{tx} is 71 nM $(k_{uncat}/((k_{cat})^{site}/K_M))$.[50]

pH−Rate Profile of D9. Figure 4 displays the variation of Michaelis−Menten parameters with pH. k_{cat}/K_M is bell shaped and has a maximum around pH 7.85, although there is a significant pH-independent activity throughout the pH range studied. K_M shows a marked increase above pH 8, and $\log(k_{cat})$ increases continuously with pH.

We assume that K_M represents a K_D for this one-step reaction with fast association of substrate relative to k_{cat}. An increase in K_M at high pH indicating lower affinity for substrate can be explained by weaker binding between the negatively charged substrate and the positively charged polymer as PEI protonation decreases under more alkaline conditions. The pH-independent component would be due to binding by guanidinium groups, which are not expected to change protonation state between pH 6.5 and 9.[31,32] Figure 4C shows the increase in k_{cat} with increasing pH for the specific base-catalyzed HPNP reaction and the reaction catalyzed by synzyme D9. The former has a slope of 1 (providing evidence that hydroxide acts as a specific

(40) Avenier, F.; Hollfelder, F. Unpublished observations.
(41) Spetnagel, W. J.; Klotz, I. M. *J. Am. Chem. Soc.* **1976**, *98* 8199−8204.
(42) Suh, J.; Scarpa, I. S.; Klotz, I. M. *J. Am. Chem. Soc.* **1976**, *98*, 7060−7064.
(43) Molenveld, P.; Stikvoort, W. M. G.; Kooijman, H.; Spek, A. L.; Engbersen, J. F. J.; Reinhoudt, D. N. *J. Org. Chem.* **1999**, *64*, 3896−3906.
(44) Manea, F.; Houillon, F. B.; Pasquato, L.; Scrimin, P. *Angew. Chem., Int. Ed. Engl.* **2004**, *43* (45), 6165−9.
(45) Suh, J.; Hong, S. H. *J. Am. Chem. Soc.* **1998**, *120*, 12545−12552.
(46) Iranzo, O.; Kovalevsky, A. Y.; Morrow, J. R.; Richard, J. P. *J. Am. Chem. Soc.* **2003**, *125* (7), 1988−93.
(47) Feng, G.; Natale, D.; Prabaharan, R.; Mareque-Rivas, J. C.; Williams, N. H. *Angew. Chem., Int. Ed. Engl.* **2006**, *45* (42), 7056−9.
(48) Kovari, E.; Kramer, R. *J. Am. Chem. Soc.* **1996**, *118*, 12704−12709.
(49) Breslow, R.; Schmuck, C. *J. Am. Chem. Soc.* **1996**, *118*, 6601−6605.
(50) Wolfenden, R. *Chem. Rev.* **2006**, *106*, (8), 3379−96.

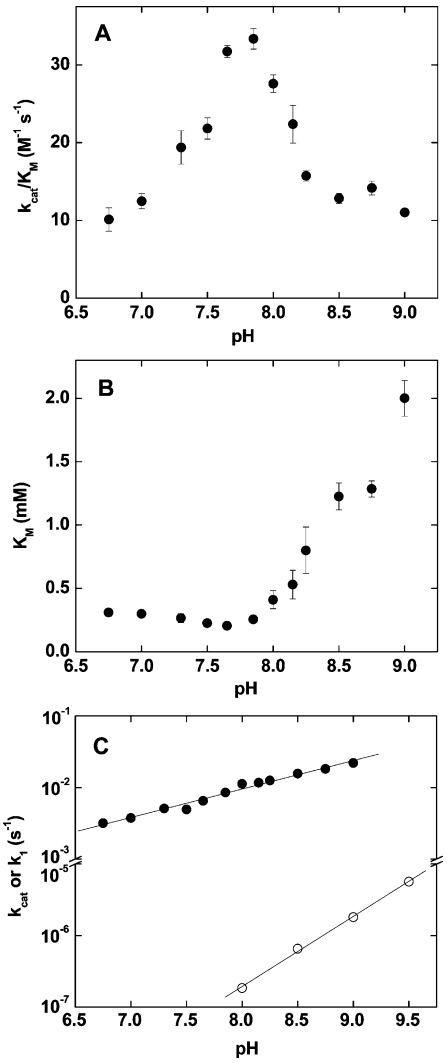

Figure 4. pH dependence of catalysis by D9. (A) Bell-shaped k_{cat}/K_M profile. (B) K_M profile. (C) k_{cat} profile (●) and, for comparison, the specific base-catalyzed background reaction (○). The slope of the uncatalyzed reaction is 0.98 ± 0.03, and that of the D9-catalyzed reaction is 0.40 ± 0.02. The Michaelis−Menten parameters were derived from plots similar to Figure 3A. Conditions: [synzyme] = 3.44 μM, [S] = 0−2 mM, 30 °C.

base),[51] but the synzyme-catalyzed reaction shows a shallower slope of 0.4, suggesting general base catalysis. However, an ambiguity exists whether the general base catalysis is due to the increase of the active ionized alcohol form of the substrate or an increase in a hypothetical active basic form of the catalyst that reacts to abstract the proton from this alcohol in the rate-determining step for the cleavage reaction. The bell-shaped k_{cat}/K_M profile reflects that the decrease in apparent binding affinity (K_M) is sharper than the increase in catalytic efficiency (k_{cat}).

Characteristics of the 'Active Site'. Although we can describe the 'active site' of this synzyme kinetically, it will never be possible to obtain the level of structural resolution familiar for many enzyme active sites. We therefore probed a range of potential anionic inhibitors to obtain information about the character of the 'active site'. Figure 5A shows that ions with different anionic charges and hydrophobicities have contrasting effects on the activity of D9. 1-Naphthyl phosphate and 4-nitrophenyl phosphate are the strongest inhibitors leading to complete inhibition with an IC_{50} of about 30 μM followed by inorganic phosphate (IC_{50} 200 μM) and ethyl-(4-nitrophenyl) phosphate ($IC_{50} \approx 500$ μM). By contrast, the inhibitory effects of other, non-phosphate inhibitors such as chloride and acetate lead to inhibition only at higher millimolar concentrations, highlighting the role of specific phosphate binding by guanidinium. Neither PEI nor PEI derivatized with guanidinium only (0.9 equiv per monomer) show any inhibition for any of the compounds mentioned above (up to 1 mM).

Inhibition data for 4-nitrophenol phosphate are replotted in Lineweaver−Burke fashion in Figure 5B and show a common intersection characteristic of competitive behavior with a K_i of 53 μM. The data for the other inhibitors (Figure S3) are displayed in Table 2. The more hydrophobic 1-naphthyl-phosphate has a tighter K_i (26 μM) than other doubly charged phosphates (4-nitrophenyl phosphate; 53 μM and inorganic phosphate; 500 μM), and single charged phosphate diester like ethyl-(4-nitrophenyl) phosphate ($K_i \approx 1$ mM) have even weaker affinities. The ability of D9 to distinguish charge, hydrophobicity, and structure of the inhibitors gives rise to competitive and other binding patterns, suggesting that the 'active sites' have a rather well-defined character.[52] Further, at a stoichiometric amount (i.e., an equal proportion of calculated active sites and inhibitor) of naphthyl phosphate (the strongest inhibitor) we observe 70% inhibition, suggesting that titration of at least a large fraction of the 'active sites' is possible and that the large extrapolation in the number of active sites is not misleading.

Hydrophobicity of the Synzyme Interior. Our derivatization protocol was targeted at creating a hydrophobic interior akin to the environment in enzyme active sites. 1-Amino naphthalene has been used to assess the hydrophobicity, e.g., of micellar environments.[53] We used this probe to characterize the microenvironment in synzyme D9. Figure 6 shows that in the presence of D9 the fluorescence maximum is shifted 10 nm compared to the fluorescence spectrum of 1-amino naphthalene in water. The spectrum with underivatized PEI is identical with the one in water, indicating that the increase in hydrophobicity is indeed a consequence of our derivatization protocol and that a synzyme with substantial hydrophobic character has been identified.

Discussion

Mechanistic Implications. Our enzyme model is proficient at binding and catalysis consistent with the following scenario.

(1) Binding. Substrate binding is driven by association of the negatively charged substrate and the positively charged synzyme. Decoration of PEI with guanidinium groups as well-known phosphate binding anchors[31,32] increases the affinity for the negatively charged phosphate substrate. The increase of binding, as measured by K_M, at lower pH (where guanidinium groups do not change protonation state) indicates that protonation of PEI amines also contributes to substrate binding. However, this effect is not just based on ion pairing, i.e., the attraction between opposite charges. The absence of strong binding for small, negatively charged ions such as chloride and acetate relative to the phosphates of equal charge (Figure 5)

(51) Feng, G.; Mareque-Rivas, J. C.; Torres Martin de Rosales, R.; Williams, N. H. *J. Am. Chem. Soc.* **2005**, *127* (39), 13470−1.

(52) Inhibition by inorganic phosphate is weakly pH dependent with a slight IC_{50} increase from 0.15 μM at pH 7 to 0.25 μM at pH 8 (see Supporting Information, Figure S3) reflecting the decreasing positive charge of the polymer. However, inhibition by naphthyl phosphate is independent of pH, highlighting that for this inhibitor pH-independent hydrophobic effects predominate over ionic effects.

(53) Sarpal, R. S.; Dogra, S. K. *J. Chem. Soc., Faraday Trans.* **1992**, *88* (18), 2725−2731.

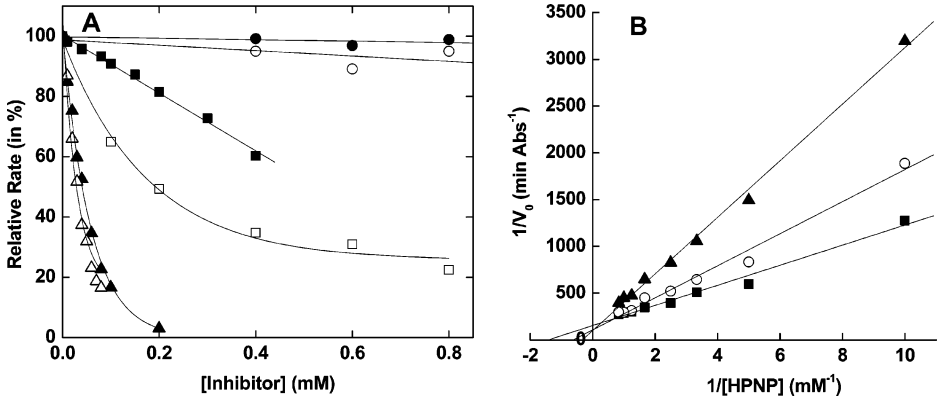

Figure 5. Inhibition profile for D9. (A) Phosphate transfer is inhibited by negatively charged molecules, such as chloride (○), acetate (●), ethyl-(4-nitrophenyl) phosphate (■), inorganic phosphate (□), 4-nitrophenyl phosphate (▲), and 1-naphthyl phosphate (△) fitted with hyperbolic decay or linear fit to guide the eyes. (B) Lineweaver−Burke representation of the inhibition of D9 by 4-nitrophenyl phosphate at 0 (■), 10 (○), and 40 μM (▲). Data are plotted as a Lineweaver−Burke representation in order to visualize the inhibition patterns, but the inhibition constants displayed in Table 2 have been calculated from more reliable nonlinear least-squares fits using the Michaelis−Menten equation. Conditions: [HEPES] = 50 mM, [synzyme] = 3 μM, 30 °C, pH 7.85.

Table 2. Comparison of the Binding Constants K_i for Inhibitors of HPNP Turnover by D9; K_M for the Substrate HPNP is 250 μM[a]

inhibitor	charge	inhibition model	K_i
1-naphthyl phosphate	2−	noncompetitive	26 ± 3 μM
4-nitro-phenyl phosphate	2−	competitive	53 ± 50 μM
inorganic phosphate	2−[b]	competitive	500 ± 220 μM
ethyl (4-nitrophenyl) phosphate	1−	noncompetitive	970 ± 86 μM
sodium chloride	1−	mixed	41 and 34 mM[c]

[a] Conditions: [HEPES] = 50 mM, [HPNP] = 0.5 mM, [synzyme] = 3.44 μM, 30 °C, pH 8. [b] At pH 8. [c] The value 41 mM refers to K_i assuming competitive inhibition and 34 mM assuming noncompetitive inhibition.

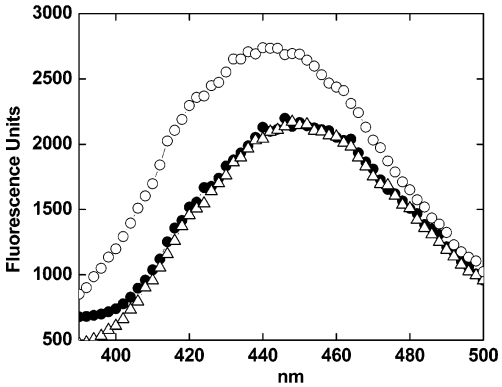

Figure 6. Fluorescence spectra of 1-amino naphthalene bound to underivatized PEI (△) and modified PEI (D9) (○) and in water (●) (excitation wavelength 340 nm). Conditions: [HEPES] 50 mM, [polymer] = 3.44 μM, [1-amino naphthalene] = 66 μM, pH 7.

suggests that the guanidinium groups recognize phosphates preferentially.[31,32,54] Hydrophobic interactions further contribute to binding, as indicated by the moderate (2-fold) enhancement of binding for naphthyl phosphate compared with 4-nitrophenyl phosphate. The occurrence of competitive binding patterns (Table 2) supports the idea that the active sites have a well-defined character that is not matched as well in the inhibitors with noncompetitive or mixed patterns. In addition to HPNP substrate, the positively charged polymer also accommodates hydroxide ions as base catalysts.

(2) Catalysis. A number of effects can bring about catalysis. (i) Acid/base catalysis. The background reaction is specific base catalyzed but does not show general base catalysis.[51] The shallower slope for the catalyzed reaction is consistent with base catalysis by unprotonated PEI amines as well as hydroxide ions that are bound to the positive PEI matrix.

A proton inventory study of an isomer of HPNP has shown that a guanidinium group in water can contribute 42-fold by acting as a general acid catalyst protonating a phosphorane-like transition state.[13] Like other hydrogen-bonding effects this one could be enhanced in a hydrophobic environment, but we have so far not been able to quantify this effect as opposed to simple electrostatic effects by a proton inventory study with D9.

(ii) Desolvation in a hydrophobic environment. The up to 193-fold observed increases in activity with higher quantities of alkyl or benzyl groups and longer alkyl chain length (Figure 2) suggest that hydrophobic effects enhance catalysis by these synzymes. For example, the activity of hydroxide can be increased by desolvation in the hydrophobic environment created by lipid modification or aprotic solvents.[55,56] In contrast to phosphate monoester hydrolysis,[56] there is no substantial solvent effect on diester hydrolysis. This can be explained by ground-state destabilization of the phosphate monoester dianion[1] that is not as readily accessible for the diester. The absence of an observed solvent effect on the ground state for diesters suggests that the effects we observed are specific to the transition state. This conclusion is consistent with the observation of charge selectivity (see below). Alternatively, desolvation of the substrate and specific medium effects are possible sources of the rate accelerations as a consequence of hydrophobic modification.

(iii) Positioning *vs* multivalent binding of hydroxide. It is possible that the hydroxide ions bound to PEI have a high effective concentration and are well positioned with respect to the substrate, but given how difficult efficient positioning has proven in other models,[57,58] this effect is likely to be small. However, the multivalent polymer can accommodate several OH^- ions, thereby increasing the availability of a large number of hydroxide ions in proximity to the bound substrate without necessarily specific positioning.

(54) Hauser, S. L.; Johanson, E. W.; Green, H. P.; Smith, P. J. *Org. Lett.* **2000**, *2* (23), 3575−8.
(55) Cox, J. R.; Ramsey, O. B. *Chem. Rev.* **1964**, *64*, 317−351.
(56) Abell, K. W. Y.; Kirby, A. J. *Tetrahedron Lett.* **1986**, *27* (9), 1085−1088.
(57) Kirby, A. J. *Angew. Chem., Int. Ed. Engl.* **1996**, *35*, 707−724.
(58) Hunter, C. A. *Angew. Chem., Int. Ed. Engl.* **2004**, *43* (40), 5310−24.

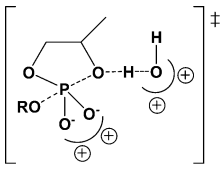

Figure 7. Likely transition-state interactions between HPNP and the synzyme matrix.

(iv) Specific stabilization of the doubly negatively charged transition state. The positive charges of guanidinium groups and the backbone ammonium groups may stabilize the negatively charged transition state. However, these effects have also been invoked above to explain the affinity of PEI derivatives for the substrate. To be catalytic, this effect has to be stronger in the transition state than in the ground state. The inhibition constants (Table 2) indicate that the phosphate compounds with two charges (and hydrophobic moieties) such as phosphate monoesters ($K_i \approx 26$ and 53 μM) bind more tightly than substrate ($K_M \approx 250$ μM) or other phosphate diesters such ethyl-(4-nitrophenyl) phosphate ($K_i \approx 1$ mM). Inorganic phosphate is doubly charged at the pH of our experiments and a weaker binder ($K_i \approx 500$ μM), which we ascribe to a lack of hydrophobic groups. Alternatively the third pK_a of phosphate could be lowered by interaction with positively charged PEI, implying that a then formally triply charged species is bound more weakly than doubly charged ones. These observations point to a scenario in which D9 is able to use differential recognition of charge to accelerate the reaction. As the transition state develops, more negative charge accumulates on the phosphoryl oxygens, resulting in a doubly negatively charged species in the extreme case of full bond making to the incoming alkoxide nucleophile (Figure 7). This double charge in the transition state is mimicked well by a phosphate monoester.[51] The comparison of K_M and the K_i for phosphate monoesters allows an estimate for the lower limit of the enhancement of the reaction due to selective stabilization of double over single charge as 5−10-fold. The actual contribution may be larger because the inhibitors are mimicking the transition state in its total charge but are not expected to be ideal mimics of its structure and charge distribution.

Most importantly, the catalytic features are a consequence of the modifications made by derivatization of PEI, validating the design of our combinatorial experiment: (a) introduction of guanidinium groups creates potential docking points for the substrate groups of phosphate and mimics enzyme active sites,[1,32] (b) creation of a hydrophobic pocket, and (c) creation of a reaction environment of high charge density. Each of these effects could be achieved by single modification of PEI. However, we observe optimal properties for combinations of reagents. For example, binding and catalysis are broadly enhanced by addition of guanidinium groups alone (see the left-hand edge of Figure 2A), but in combination with other modification, this effect on catalysis is approximately 200-fold higher (Figure 2A) than without hydrophobic modifications.

This finding implies that providing a hydrophobic and polar microenvironment enhances molecular recognition. The observed characteristics can be rationalized as a function of the modification made to the polymer. Just as in a directed evolution experiment (e.g., in high-throughput screening of protein mutants), the features of the catalyst D9 reflect the multiple turnover conditions under which the catalysts were screened.

Comparison to Other Phosphate Transfer Models. Often molecular recognition studies are conducted in organic, aprotic solvents rather than water. This is partly due to solubility considerations, but molecular recognition features are also much easier to engineer in the absence of interfering hydrogen-bonding competition from water. Bis(alkylguanidinium) catalysts[10] show the best reported rate enhancement for metal-free phosphate transfer catalysis so far ($k_{cat}/k_{uncat} \approx 290$), but work has been in aprotic acetonitrile only. By contrast, the binding features of our synzymes are sustained in water. Two other models, a cyclodextrin[9,49] and a recently reported sapphyrin[11] (a porphyrin-like macrocycle with attached potential alcohol nucleophiles), show activity in water with rate accelerations k_{cat}/k_{uncat} of 140 and approximately 20,[59] respectively. Tris(2-aminobenzimidazoles) have been shown to hydrolyze the much less reactive substrate RNA,[12] but no rate acceleration has been determined.

The effective rate acceleration k_{cat}/k_{uncat} of 46 800 for this model is two orders of magnitude beyond previous models and calculated per active site ($(k_{cat})^{site}/k_{uncat}$) faster by one order of magnitude.[60] The strong binding to the polycationic PEI framework leads to relatively low K_M values, so the catalytic proficiency $(k_{cat}/K_M)/k_2$[61] is likewise enhanced by up to three orders of magnitude over previous models. The detailed data are summarized in Table 1.

Other models for metal-free phosphate transfer are less proficient at multiple turnover (<2) than our model (180 turnovers per site, 2340 overall). The ability to recognize doubly charged species selectively may be responsible for the larger number of turnovers observed for D9. The products are singly charged and thus bind more weakly to the PEI derivative than the transition state, reducing product inhibition. Furthermore, the monoanionic product has also lost a hydrophobic group (4-nitrophenolate), resulting in weakened binding to the hydrophobic modifications groups.

Table 1 also lists the kinetic data obtained for some of the best enzyme models containing a catalytic metal that have been studied for the reaction of HPNP. Despite the high reactivity of the metal ion, the best calixarene[43] and dinuclear complexes[47] containing two Zn^{2+} ions have catalytic proficiencies that are only one order of magnitude higher, and other models are in the same region[44] or weaker[45,46] (including a nickel-containing synzyme[45]). Thus, synzyme D9 is not only the best metal-free catalyst for HPNP cleavage, but its efficiency is comparable with that of a previous metalated synzyme[45] and only one order of magnitude lower than the best metal complexes.[43,44,46] The tight binding observed up to pH 8 ($K_M = 0.25$ mM) generates a very good enzyme proficiency comparable with the metallic systems. Collectively, these data suggest that D9 is almost as good as a metal at providing a reactive dynamic interface for phosphate transfer. However, although part of a class of difficult reactions, HPNP transesterification involves departure of a good leaving group and an *intra*molecular group acts as the catalytic nucleophile. In their current stage of development, derivatized PEIs (as well as the other models discussed above) are not able to provide such a precisely positioned nucleophile directly

(59) On the basis of the extrapolation of the measured rate ($k_{uncat} = 1.1 \times 10^{-10}$ s^{-1}) at pH 6.6, 20 °C to pH 7.5 (×10), 37 °C (×4) (k_{uncat} extrapolated = 4.4×10^{-9} s^{-1}).

(60) Fitting the data to a saturation curve when the saturation level is not well defined (as in Figures 3A and S1) will lead to an underestimation of $(k_{cat})^{site}$ and thus an underestimation of $(k_{cat})^{site}/k_{uncat}$.

(61) We calculate $k_2 = k_{uncat}/1$ M (assuming 1 M catalyst).

attached to the catalyst. This may limit efficient catalysis to intramolecular reactions.

Conclusions

Synzyme D9 integrates a complete set of characteristics typical of an enzyme. The observation of saturation kinetics and the existence of specific cognate inhibitors that can act competitively resemble the features of an enzyme active site. D9 also exhibits multiple turnovers, distinguishing this model from previous nonmetallic phosphate transfer catalysts, all of which show only single turnover. D9 is thus a true catalyst as opposed to a stoichiometric reagent. As in naturally evolved enzymes, a compromise is struck between two effects that are optimized at the pH at which screening was carried out, resulting in a bell-shaped pH−rate profile for k_{cat}/K_M familiar from enzymatic systems. This process is equivalent to evolution under a given set of in vivo conditions.

The approach of modifying a polymer with mixtures of suitable catalytic groups at a high effective concentration demonstrates that a fairly unsophisticated catalyst that combines simple binding features and exploits hydrophobic effects for catalysis can be surprisingly efficient.

More generally, the observation that the efficiency of the simple modified dynamic polar interfaces of PEI almost matches the efficiency of models with a metal-ion cofactor (that would normally be considered to be much more reactive) may have implications for early evolution. It demonstrates that a simple phosphate binding motif, in conjunction with a hydrophobic environment, can provide a selective catalytic advantage as a starting point for further evolutionary improvements. This means that two potential avenues for phosphate transfer catalysis—with and without a metal—should be considered in speculation about events in the early evolution of primordial catalytic systems.

Materials and Methods

All reagents and solvents were purchased from commercial sources and used as received. The barium salt of 2-hydroxypropyl-4-nitrophenyl phosphate (HPNP) was synthesized according to literature procedures.[30]

Synzyme Synthesis. In a preliminary study we established that guanidylation reactions used for PEI modification were quantitative under these conditions by reacting diethylene triamine ($[H_2NCH_2CH_2]_2$-NH) with 1*H*-pyrazole-1-carboxamidine and *N*,*N*-diisopropylethylamine in DMF (25 mL) for 2 h. The resulting white solid, recrystallized from methanol/ether, corresponded to *N*,*N*‴-(iminodiethylene)bisguanidine dihydrochloride ($[H_2N(HN{=})CNHCH_2CH_2]_2NH{\cdot}2HCl$). ESI-MS: M + 2HCl (100%, 259 Da, calcd 259.108). ^{1}H NMR (D_2O): δ 2.65 (t, 4H, CH_2), 3.16 (t, 4H, CH_2). ^{13}C NMR (D_2O): δ 40.58 (s), 46.61 (s), 156.96 (q). Thus, only primary amines were derivatized by this reagent combination. Commercial PEI (25 kDa, Sigma) was dissolved in DMF to give a final PEI concentration of 20.5 mg mL^{-1} (0.488 M in monomer residues). For guanidylation, freshly prepared solution mixtures of 1-*H*-pyrazole-1-carboxamidin hydrochloride and *N*,*N*-diisopropylethylamine (1:1, 0−0.2259 M total concentration) were made up in DMF. These solutions (0.6 mL) were added under vigorous stirring (using a microstirring bars with a diameter of 2 mm × 5 mm; Aldrich) to aliquots of 0.6 mL of the PEI solution (to give a guanidylation ratio of 0−2 per primary amine) in 96-well, 2.2 mL polypropylene plates (ABgene, U.K.). These reaction mixtures were left under stirring overnight at room temperature. For alkylation, freshly prepared solutions of benzyl bromide and dodecyl iodide mixtures (1:1, 0−1.84 M) were then added (0.2 mL) under vigorous stirring to give alkylation ratios from 0 to 2 equiv per monomer residue. Stirring was continued for 4 days at room temperature.

Synzymes selected for detailed study after initial screens were synthesized on a larger scale in 50 mL Falcon tubes. Crude reaction mixtures were diluted (1:2) into hydrochloric acid (50 mM) and transferred to a dialysis tube (Spectra/Por membrane, M_w cutoff 14 000). The resulting solutions were dialyzed under slow stirring against each of the following buffers for at least 2 h: 20% EtOH in 50 mM HCl; 50 mM HCl; distilled water (twice); 50 mM NaOH (twice) and water (three times). To remove metals, the synzymes were dialyzed against Chelex beads in deionized distilled water (Milli-Q Triple Red), and all solutions were handled in plastic flasks containing Chelex beads. Detailed kinetic parameters were determined after extensive dialysis.

All synthetic procedures were carried out more than once and reproducibly gave catalysts with kinetic properties within 20% of the values described.

Kinetic Measurements. Reactions of **1** were monitored by following the increase in absorbance at 405 nm (corresponding to the release of 4-nitrophenolate) in 96-well plates (NUNC) in a microtiter plate reader (Molecular Devices Spectramax Plus or a BMG Labtech Fluostar Optima). The 96-well plates were thermosealed with an optically transparent film (Clear Seal Diamond, ABgene, U.K.) in order to avoid evaporation during the measurements. To exclude the effects of metals, kinetics were conducted with and without EDTA (0.1 mM). The following buffers were used (50 mM): MES (2-(*N*-morpholino)-ethansulfonic acid, pH 6.0−6.5), HEPES (*N*-(2-hydroxyethyl)piperazin-*N*′-2-ethansulfonic acid, pH 6.75−8.25), and CHES (2-(*N*-cyclohexylamino)ethansulfonic acid, pH 8.5−9.0) at 30°C.

For initial library screening, aliquots of the synzyme reaction mixtures (50 μL) were diluted in DMF to 200 μL. This solution was quenched with aqueous sodium hydroxide solution (800 μL, 50 mM NaOH) and allowed to stand for 20 h. This solution (30 μL, final concentration 8.75 mM in PEI monomer residues) was added to 110 μL of HEPES buffer (pH 8.0) and incubated (10 min, 30 °C), and HPNP (10 μL, final concentration 1 mM) was added (total volume 150 μL).

For detailed kinetic characterization resynthesized, extensively dialyzed, synzyme D9 stock solutions (3.44 μM in polymer) were used for kinetic measurements with [HPNP] = 0−2 mM. Several batches of synzyme D9 had essentially identical activity (within 10%). ^{31}P NMR spectra during reaction showed only the starting material 1 (∂_P −3.9 ppm) and the expected cyclic phosphate ester **2** as the product (∂_P 19.2 ppm).[62] Initial velocities were calculated from the linear part of the absorbance increase at 405 nm (<5% of substrate consumed), plotted against the substrate concentration $[S_0]$ to obtain the Michaelis−Menten plot using a standard fit ($v = [E_0](k_{cat})^{total}[S_0]/([S_0] + K_M)$). The extinction coefficient for a fixed path length $\epsilon_{405}d$ was determined at different pH values (e.g., $\epsilon_{405}d$ was 3665 M^{-1} at pH 7). For inhibition experiments, sodium chloride, sodium acetate, inorganic phosphate, naphthyl phosphate, ethyl-(4-nitrophenyl) phosphate, or 4-nitrophenyl phosphate were incubated for 10 min with the dialyzed PEI in buffer at 30 °C before addition of HPNP.

To determine rate accelerations for a single active site $(k_{cat})^{site}$ experiments were performed at $[S_0][dlt]$[synzyme], where the first-order rate of reaction could be determined under single-turnover conditions (Figure 3B).[28,29,41,42] Reactions were followed in a VARIAN CARY-100 spectrophotometer with [HPNP] = 25 μM and [synzyme] = 0−12.6 μM. The limited solubility of the synzymes precluded measurements at higher concentrations. The apparent first-order rate constants (k_{obs}) were plotted against the polymer concentration $[E_0]$. The saturated level of this curve (extrapolated from a fit to $k_{obs} = (k_{cat})^{site}[E_0]/([E_0] + K_M)$) was taken as $(k_{cat})^{site}$. The number of active site per polymer molecule was calculated by dividing $(k_{cat})^{total}$ by $(k_{cat})^{site}$.

(62) Oost, T.; Filippazzi, A.; Kalesse, M. *Liebigs Ann. Chem.* **1997**, 1005−1011.

Acknowledgment. F.A. is a Marie-Curie fellow of the European Union. J.B.D. thanks CONACYT for a postdoctoral fellowship. L.D.V. thanks St. John's College for a Benefactors' Scholarship and the Cambridge European Trust for support. This research was supported by the EPSRC.

Supporting Information Available: Determination of the number of active sites per polymer near the optimum pH (Figure S1); Lineweaver−Burke representation of the inhibition of D9 by different inhibitors (Figure S2); inhibition profile for D9 with 1-naphthyl phosphate and inorganic phosphate depending on pH (Figure S3). This material is available free of charge via the Internet at http://pubs.acs.org.

JA069095G